Folding Dynamics of β-Hairpins: Molecular Dynamics Simulations

Jinhyuk Lee, Soonmin Jang, Youngshang Pak,† and Seokmin Shin*

School of Chemistry, Seoul National University, Seoul 151-747, Korea
†Department of Chemistry, Pusan National University, Pusan 609-735, Korea
Received February 28, 2003

We have studied the folding mechanism of β-hairpins from proteins of 1GB1, 3AIT and 1A2P by unfolding simulations at high temperatures. The analysis of trajectories obtained from molecular dynamics simulations in explicit aqueous solution suggests that the three β-hairpin structures follow different mechanism of folding. The results of unfolding simulations showed that the positions of the hydrophobic core residues influence the folding dynamics. We discussed the characteristics of different mechanisms of β-hairpin folding based on the hydrogen-bond-centric and the hydrophobic-centric models.

Key Words : Protein folding, Molecular dynamics, β-Hairpin, Unfolding mechanism, Hydrophobic cluster

Introduction

In the wake of the completion of decoding human Genome, one of the most important and challenging problems in biological sciences is to understand and predict the "protein-folding", *i.e.* the spontaneous formation of native structures of functional proteins starting from the given amino acid sequences. New experimental techniques have provided much information on the details of the events that occur during the folding process.[1,2] Theoretical and computational studies of simplified models have provided general insights into the specific features of folding mechanism and the properties of folding free-energy landscapes.[3-6] Predicting the native structures of proteins from amino-acid sequences alone is a long-standing challenge, which has great practical significance as well as considerable scientific interest. Such *ab initio* structure prediction or protein-folding may require the ability to describe the whole folding process at the level of atomic precision, which is still not feasible despite rapid advances in the field.[7]

Understanding the mechanism of formation of basic structural elements such as α-helices and β-sheets can provide useful information for the folding of larger proteins. α-helix formation has been extensively investigated both experimentally and theoretically.[8,9] In contrast, the formation of β-sheet structures has not been studied in detail. It has been proposed that β-turns and β-hairpins act as initiation sites in early protein folding events.[10,11] A β-hairpin is the simplest form of anti-parallel β-sheet structure and is defined by a loop region flanked by two β-strands. Recent studies suggested that the positioning of the side chain groups in such a way as to promote the formation of a hydrophobic cluster is essential for the folding of hairpin structures. Concerning the detailed pictures of hairpin formation, especially with respect to the relative timing of the formations of the interstrand hydrogen bonds near the turn and the hydrophobic core, two different mechanisms of β-hairpin folding have been proposed. Muñoz *et al*. studied the kinetics of folding a 16-residue β-hairpin from protein GB1 using a nanosecond laser temperature-jump technique.[12] They suggested that the formation of β-hairpin from protein GB1 is initiated from the β-turn which then "zips up" the remaining native hydrogen bonds. A turn stabilized by interstrand hydrogen bonds positions the aromatic residues so that they are poised to pack into a hydrocarbon cluster. Bonvin and van Gunsteren studied the stability and folding of the 19-residue β-hairpin fragment of the α-amylase inhibitor tendamistat.[13] Several unfolding and refolding simulations suggested a model for β-hairpin formation in which the turn is formed first, followed by hydrogen bond formation closing the hairpin, and subsequent stabilization by side-chain hydrophobic interactions. Prevost and Ortman performed refolding simulations of a β-hairpin fragment of barnase using a simulated annealing method.[14] They found that interstrand side-chain compactness and backbone hydrogen bonding provide concurrent stabilizing factors for the β-hairpin formation.

Pande and Rokhsar studied the unfolding and refolding pathway of a β-hairpin fragment of protein GB1 using molecular dynamics simulations.[15] It was suggested that the high-temperature unfolding of the β-hairpin undergoes a series of sudden discrete conformational changes. According to their results, the hydrophobic cluster would form without assistance from the interstrand hydrogen bonds, suggesting that the β-hairpin refolds by the "hydrophobic collapse" mechanism. In this model, the hairpin collapses to a compact structure associated with a "molten globule". The driving force towards the compact structure is global and in general nonspecific (a hydrophobic interaction). In the next step, "mistakes" in the compact structure are corrected by forming native hydrogen bonds. The reorientation of the compact structure is relatively slow and resembles the transition from a molten globule state to the native state of the protein. Dinner *et al*. obtained the free energy surface and conformations involved in the folding of the same β-hairpin from

*Corresponding Author. Fax: +82-2-889-1568; E-mail: sshin@snu.ac.kr

multicanonical Monte Carlo simulations.[16] Their results suggested that folding proceeds by a collapse leading to the formation of the hydrophobic assembly; subsequently, the hairpin hydrogen bonds propagate outwards in both directions from the hydrophobic core. Ma and Nusssinov studied the contributions of three components of a β-hairpin peptide: turn, backbone hydrogen bonding, and side-chain interactions.[17] They examined the structural stability of the β-hairpin under systematic perturbations of the turn region, backbone hydrogen bonds and the hydrophobic core formed by the side-chains. Their results support a side-chain-centric view of the folding of a hairpin structure. For small peptides and proteins, the disruption of the hydrophobic core appears to be one of the major steps in the folding/unfolding process.

Typical molecular dynamics simulations can examine the trajectories of proteins up to tens of nanoseconds. The time scales of protein folding in the micro- to millisecond range are still not really accessible to direct simulation studies. One fruitful approach is to investigate protein unfolding by performing simulations under strongly denaturing conditions (high temperature and/or pressure). These simulations can provide insights into the early stages of unfolding, which are assumed to reflect the later stages of refolding under native conditions.[18-20] We note that there remain important open questions concerning the relationship between unfolding at high temperatures and the folding process at physiological temperatures.[21-23]

In the previous study,[24] we investigated the mechanism of formation of a 16-residue β-hairpin from the protein GB1 using molecular dynamics simulations in an aqueous environment. The analysis of unfolding trajectories at high temperatures suggests a refolding pathway consisting of several transient intermediates. The changes in the interaction energies of residues are related to the structural changes during the unfolding of the hairpin. In a subsequent study,[25] essential dynamics (ED) and generalized 2D correlation analysis were performed on the trajectories of unfolding simulations at different temperatures. The results of the 2D correlation analysis illustrate the correlated structural changes as the temperature is increased. The asynchronous 2D correlation spectrum reveals the existence of sequential events in the unfolding of the peptide. The order of structural changes suggested by such an analysis support the hydrophobic collapse mechanism of folding for the β-hairpin fragment of protein GB1.

It is interesting to note that the three hairpins from proteins GB1 (PDB entry 1GB1 : 16 residues), tendamist (PDB entry 3AIT : 19 residues), and barnase (PDB entry 1A2P : 18 residues) seemed to show different folding mechanism. It is noted that the positions of the large (hydrophobic) side-chains are different in the three cases (Fig. 1). In the β-hairpin of protein GB1, the hydrophobic residues are located in the middle of the two strands, while the β-hairpin of tendamistat (3AIT) has the hydrophobic residues clustered near the turn (loop) region. The hydrophobic residues of the hairpin of barnase (1A2P) are spread out over the peptide. One may argue that the positions of the hydrophobic core are important in determining folding mechanism of hairpins. In the present study, we have studied unfolding of the β-hairpins from the above three proteins by MD simulations in explicit water solvents at several temperatures. Unfolding trajectories are analyzed by calculating the order parameters such as the number of hydrogen bonds and the radius of gyration. Further insights into the detailed mechanism of β-hairpin (un)folding are obtained by examining the interaction energies analysis, the secondary structure evolution, and the two-dimensional correlation analysis based on the essential dynamics (ED) analysis.

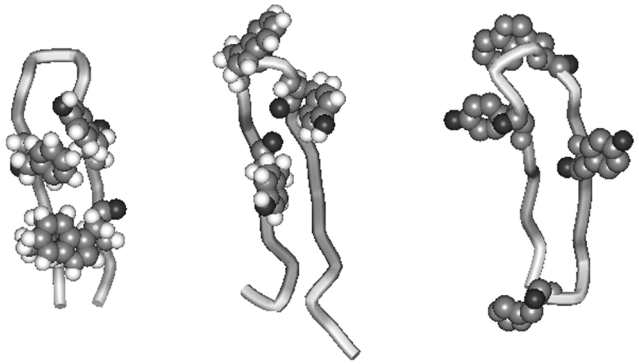

Figure 1. Native structures of the β-hairpin fragments from (a) the protein GB1 (residues 41-56 of 1GB1), (b) the α-amylase inhibitor tendamistat (residues 10-28 of 3AIT), and (c) the barnase (residues 85-102 of 1A2P). The side chains of hydrophobic residues [(Trp43, Tyr45, Phe52, Val54) of 1GB1; (Tyr15, Trp18, Tyr20) of 3AIT; and (Tyr90, Trp94, Tyr97, His102) of 1A2P] are shown in space-filling mode.

Model and Simulation Details

The three hairpin structures were obtained from the respective PDB entries. Figure 1 shows the native structures of the three hairpins where the hydrophobic residues with large side-chain groups are represented by space-filling models. The hydrophobic residues are as follows: 1GB1 (3TRP 5TYR 12PHE 14VAL); 3AIT (6TYR 9TRP 11TYR); 1A2P (6TYR 10TRP 13TYR 18HIS). We also identify the bend turn regions of the hairpins as follows: 1GB1 (6th-11th residues), 1A2P (6th-12th residues) and 3AIT (7th-12th residues). The hairpin of 3AIT has one S-S bond between two terminal cysteine residues. The simulations of the 3AIT hairpin were performed without S-S bond.

All simulations were performed using the recent version (v.27) of CHARMM package with the CHARMM all-H potential.[26] Initial structures obtained from PDB were minimized with ABNR method and placed in the cubic box with TIP3P waters. In the equilibrium simulations, the temperature of the system is raised from 0 K to a specific temperature. Three independent simulations of 2 *ns* duration have been carried out for each of five different temperatures (300, 400, 500, 600 & 700 K). A time step of 1 fs was used and the trajectories were saved every 1 *ps*. To analyze the

trajectories, we calculated several quantities as order parameters: the number of hydrogen bonds (N_{HB}) and the radius of gyration of the whole peptide (R_G). These order parameters are expected to reflect the compactness of the protein structure and give information about the intermediate states of unfolding. N_{HB} was calculated with the SIMLYS program.[27] A hydrogen bond was defined by the bond angle (*N–H–O*) being restricted in the range between 135° and 180° with the bond distance being less than 3.3 Å. R_G was alculated with the modified program of SITUS developed by Wriggers *et al.*.[28] Secondary structure contents of the peptides were calculated using the SECSTR module of the program PROCHECK.[29]

The overall interaction energy and the corresponding force for each residue in a protein can be decomposed into various components.[30] The relative importance of these components can be correlated with conformational changes during the (un)folding of proteins. In the previous work,[24] we showed that the electrostatic components can reflect the structural changes associated with the loss of backbone hydrogen bonding and the van der Waals components are related with the disruption of the hydrophobic core of a protein. We have developed a method for calculating different components of the interaction energy or force for each residue in a protein. For instance, (1) van der Waals (*evdw*), (2) electrostatic (*eelec*), and (3) total (*etot*) interaction energies of each residue with the rest of the protein molecule and solvent molecules can be obtained.

The essential dynamics method[31] is based on the diagonalization of the covariance matrix built from atomic fluctuations in an MD trajectory from which overall translation and rotations have been removed. The coordinates of the C_α atoms are used for the analysis. Diagonalization of the covariance matrix yields a set of eigenvectors and eigenvalues, which are sorted by the size of the eigenvalue. The basic idea of essential dynamics is that only the correlated motions represented by the eigenvectors with large corresponding eigenvalues are important in describing the overall motion of the protein. For each temperature, MD trajectories of three separate simulations are concatenated to form one big trajectory and a covariance matrix is constructed. The resulting eigenvectors now indicate the concerted motions of atoms, which are common to the separate trajectories. The mean square fluctuations reveal structural changes during unfolding trajectories. The essential dynamics analysis was carried out using the WHAT IF modeling program.[32]

Noda and coworkers have proposed perturbation-based 2D correlation spectroscopy, which utilizes an additional external perturbation applied during the spectroscopic measurement to stimulate the system of interest.[33,34] The response of the system to the applied perturbation leads to characteristic variations in the spectrum, which is often called a "dynamic spectrum". A simple scheme of correlation analysis can be applied to a series of perturbation-induced dynamic spectra, collected in some sequential order, yielding desired 2D correlation spectra. The dynamic spectra can be obtained as a function of the quantitative measure of the imposed external perturbation such as temperature, pressure, concentration, stress, or electric field. In the present study, the dynamic spectrum corresponds to the mean square fluctuations as a function of residue number, obtained from the ED analysis at a specific temperature. The 2D spectrum represents correlations in the structural changes due to temperature increase (*i.e.* unfolding) for the two different regions of the peptide. The intensity of a synchronous 2D correlation spectrum represents the simultaneous changes of the spectral intensity variations during the interval of the external perturbation. The asynchronous 2D correlation spectrum has no autopeaks and is anti-symmetric with respect to the diagonal line. An asynchronous cross peak develops only if the intensities of two spectral features change out of phase. The detailed methods for calculating and interpreting correlation spectra are explained in the previous work.[25]

Results and Discussion

We have performed molecular dynamics (MD) simulations of the unfolding of the three types of β-hairpin structures using CHARMM all-H potential. The hairpins will be referred to the PDB entries (1GB1, 3AIT, 1A2P). At high temperatures such as 600 K and 700 K, the trajectories of the simulations usually result in a completely unfolded state within the simulation times (2 *ns*), while the folded states

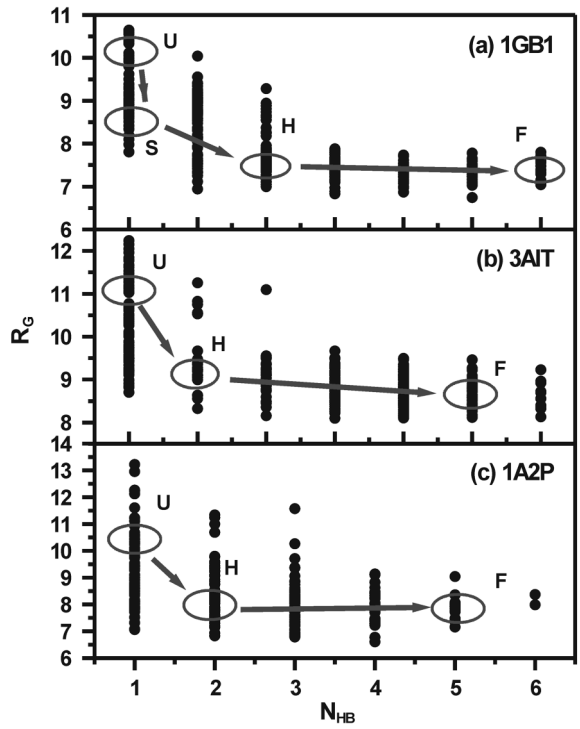

Figure 2. Two-dimensional plot in the space of N_{HB} and R_G, which represents conformations of the hairpins observed during unfolding simulations for (a) 1GB1 at 400 K, (b) 3AIT at 400 K, and (c) 1A2P at 500 K. Circles indicate representative conformations corresponding to the states identified as the "folded" (*F*), the "hydrophobic core" (*H*), the "partially solvated cluster" (*S*), and the "unfolded" (*U*) states.

with native-like structures are maintained during the simulations at room temperature (300 K). At an intermediate temperature (400 K or 500 K), partial unfolding and refolding of the hairpins are observed in typical trajectories. We calculated the number of backbone hydrogen bonds (N_{HB}) and the radius of gyration (R_G). The time evolution of N_{HB} and R_G can reveal the structural changes involved in unfolding/refolding dynamics. In the previous studies,[15,24] it was suggested that the high-temperature unfolding of a β-hairpin undergoes a series of sudden discrete conformational changes between states identified as the "folded" (*F*), the "hydrophobic core" (*H*), the "partially solvated cluster" (*S*), and the "unfolded" (*U*) states. The states *H* and *S* are transient kinetic intermediates. In Figure 2, we showed two-dimensional plots in the space of N_{HB} and R_G, which represents conformations of the hairpins observed during unfolding simulations at an intermediate temperature (1GB1 and 3AIT at 400 K; 1A2P at 500 K). The results are consistent with the unfolding mechanism with reversible interconversions ($F \leftrightarrow H \leftrightarrow (S) \leftrightarrow U$). It is noted that discriminating the *H* and *S* states based on N_{HB} and the radius of gyration is sometimes difficult.

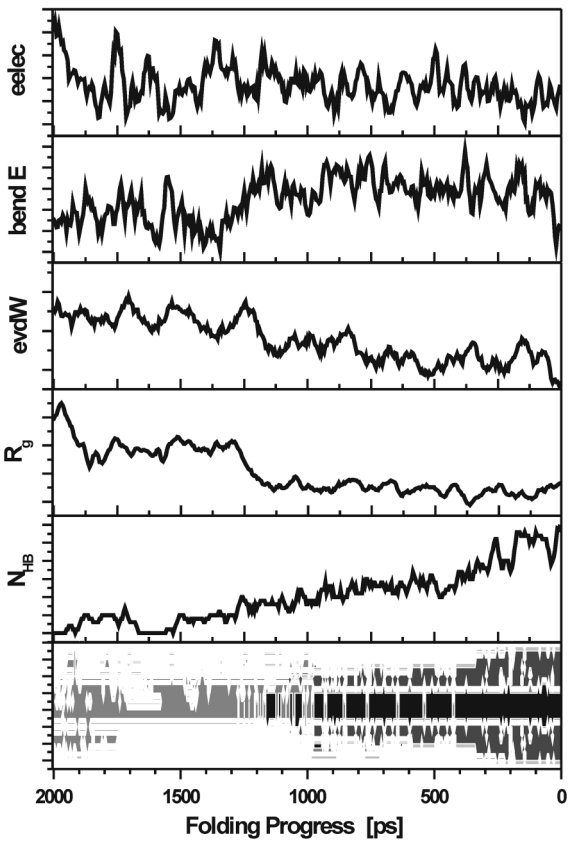

Figure 3. The evolution of several quantities for the hairpin from 1GB1 as a function of *folding progress* as defined by the reverse of the unfolding trajectory at 400 K. The first panel displayed the evolution of the secondary structures of the hairpin: hydrogen-bonded turn structure (black); beta-ladder structure (dark gray); bend structure (gray); extension of beta-strand & isolated beta-bridge (light gray. Interaction energy analysis gives the vad der Waals interaction energies of the hydrophobic core (*evdW*); the electrostatic energies of the bend region (*bendE*); and the electrostatic energies of the whole hairpin (*eelec*).

In Figure 3, we showed several quantities of the hairpin from 1GB1 as a function of *folding progress* which is defined as the reverse process of the unfolding. The calculations were done on one of the representative trajectories at 400 K. The first panel displayed the evolution of the secondary structures of the hairpin. The bend structure (gray) in the turn region, which is stabilized by the electrostatic interactions between the two strands, appeared in the early stage of folding. As the fraction of the native hydrogen-bonding increases, the hydrogen-bonded turn structure (black) is formed followed by the formation of beta-ladder structure (dark gray) in the strand region. The behavior of the radius of gyration (R_G) indicated that the hairpin collapsed in the very early folding progress, which is closely correlated with the decrease (more negative) in the electrostatic interactions of the whole peptide. In Figure 4, the evolution of the total energy of the 1GB1 hairpin during (un)folding is shown along with the designation of four important structures involved in the folding process. Starting from the unfolded structure (*U*), the electrostatic interactions of the whole hairpin lead to a compact structure, so called *solvated structure* (*S*). The solvated structure has R_G value of about 8-9 Å with negligible native hydrogen-bonding. Similar intermediate local minimum structures, which are mostly stabilized by the electrostatic interactions of bend residues, occurred after the first formation of the solvated structure. The stabilization due to the hydrophobic interactions of the hairpin strand results in the *hydrophobic collapse structure* (*H*). The formation of *H* structure involves sharp decreases in R_G and the hydrophobic interactions of hydrophobic core residues (Fig. 3). The hydrophobic collapse structure has R_G value of about 7.5 Å with few (~2) native hydrogen bonds. The transformation of *S* to *H* structures may be aided by electrostatic interactions of bend

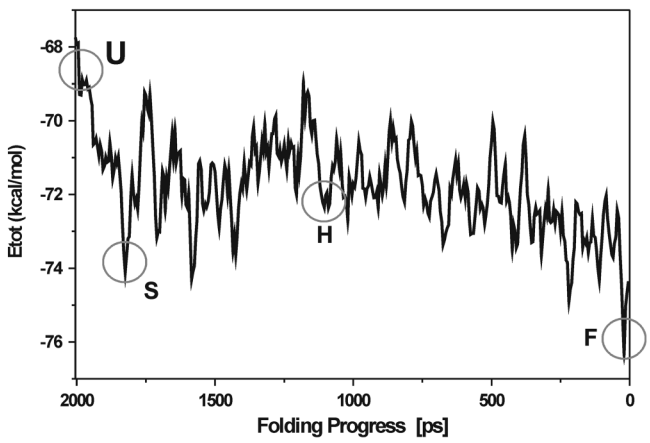

Figure 4. The evolution of the total interaction energies (*Etot*) per residue for the hairpin from 1GB1 as a function of *folding progress* as defined by the reverse of the unfolding trajectory at 400 K. Circles indicate representative conformations corresponding to the states identified as the "folded" (*F*), the "hydrophobic core" (*H*), the "partially solvated cluster" (*S*), and the "unfolded" (*U*) states.

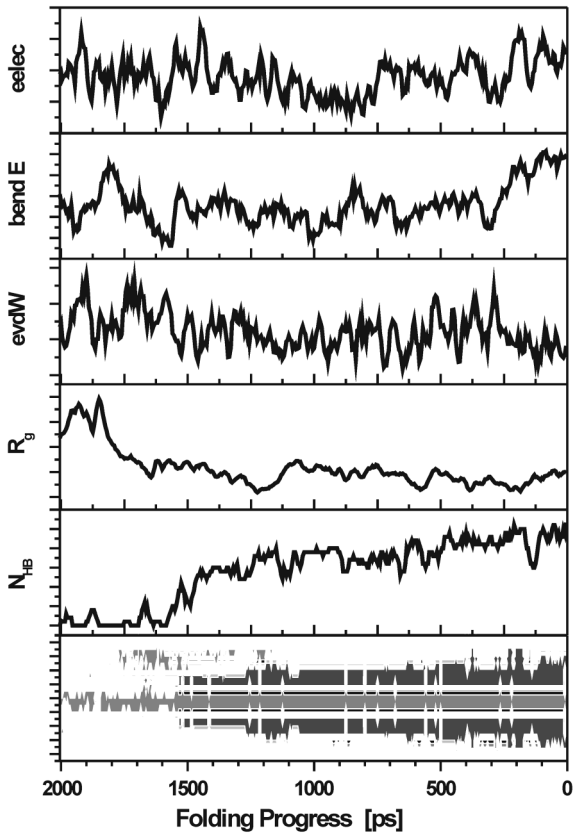

Figure 5. The evolution of several quantities for the hairpin from 3AIT as a function of *folding progress* as defined by the reverse of the unfolding trajectory at 400 K. The first panel displayed the evolution of the secondary structures of the hairpin: hydrogen-bonded turn structure (black); beta-ladder structure (dark gray); bend structure (gray); extension of beta-strand & isolated beta-bridge (light gray. Interaction energy analysis gives the vad der Waals interaction energies of the hydrophobic core (*evdW*); the electrostatic energies of the bend region (*bendE*); and the electrostatic energies of the whole hairpin (*eelec*).

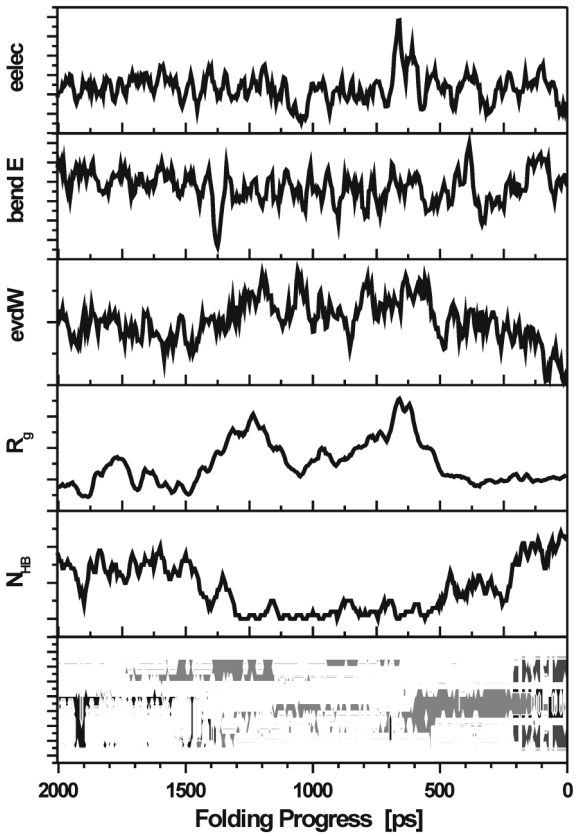

Figure 6. The evolution of several quantities for the hairpin from 1A2P as a function of *folding progress* as defined by the reverse of the unfolding trajectory at 500 K. The first panel displayed the evolution of the secondary structures of the hairpin: hydrogen-bonded turn structure (black); beta-ladder structure (dark gray); bend structure (gray); extension of beta-strand & isolated beta-bridge (light gray. Interaction energy analysis gives the vad der Waals interaction energies of the whole hairpin (*evdW*); the electrostatic energies of the bend region (*bendE*); and the electrostatic energies of the whole hairpin (*eelec*).

regions or hydrophobic interactions of hydrophobic core residues. The number of hydrogen bonds gradually increases as the *folded structure* (*F*) is formed from *H*. About four more hydrogen bonds are formed in such final *tune-up* process. The $H \rightarrow F$ transformation can be seen from the gradual decrease in the total electrostatic interactions of the hairpin (Fig. 3).

The evolution of several quantities of the hairpin from 3AIT during (un)folding at 400 K is displayed in Fig. 5. The hairpin has three hydrophobic residues (6TYR 9TRP 11TYR) and the presence of two hydrophobic residues in the turn region precludes the formation of hydrogen bonds. In the turn region, mostly the bend structure (gray) is observed instead of the hydrogen-bonded turn structure (black). Because there are no large hydrophobic residues in the strand, the intermediate structures similar to solvated structure (*S*) in 1GB1 hairpin cannot be stabilized in the case of 3AIT. There is no sharp change in the hydrophobic (vdW) interactions. In this case, the decrease of the radius of gyration is correlated with the electrostatic interactions in the turn region. After the bend region is stabilized, the gradual formation of native hydrogen bonds in the strand region constitutes the final tune-up process of folding. These results are consistent with so-called *zip-up* mechanism of hairpin folding. Figure 6 shows the same analysis as above for the hairpin from 1A2P concerning unfolding simulations at 500 K. The hairpin has higher folding temperature than the other two hairpins, which may be due to the formation of a closed form by terminal hydrophobic residue (HIS).[14] 1A2P hairpin doesnt support a compact structure as in the case of 3AIT hairpin. Although the structures in the later stage of unfolding trajectory (2000-1500 *ps*) seem to have small R_G and large N_{HB}, the secondary structure analysis showed that they are different from native structures. Only in the time range of 700-0 *ps*, the formation of the native structure is observed. It is noted that the decrease of R_G and the formation of hydrogen bonds occur simultaneously as the folding progressed. The same trends are reflected in the simultaneous decreases of the hydrophobic and electrostatic interactions. It can be argued that the formation of turn and

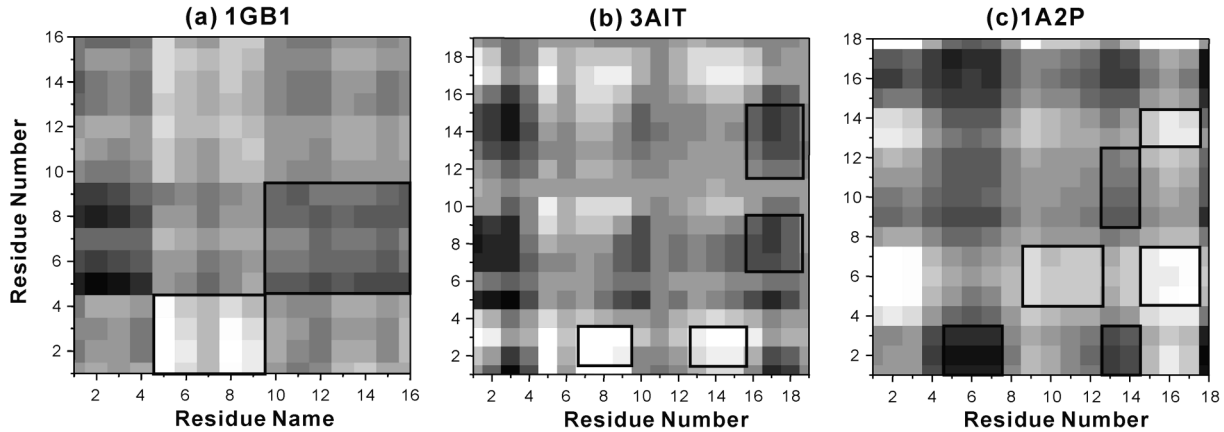

Figure 7. Asynchronous 2D correlation spectra for the three hairpins from (a) 1GB1, (b) 3AIT, and (c) 1A2P. The color scales are from +1.0 (black) to −1.0 (white). Solid boxes are drawn to highlight different off-diagonal regions important for determination of sequential changes of structures during unfolding.

the hydrophobic collapse are occurring concurrently for this hairpin structure.

Using the combined trajectories of the three separate simulations, essential dynamics analysis was performed to examine the changes in the dynamical structures of the peptide at different temperatures. As in the previous studies,[25,30,35] only a few eigenvectors are found to represent the essential motions in the peptide. The generalized 2D correlation analysis has been performed using the displacements from the ED analysis as input data for generating the synchronous and asynchronous plots. These plots represent the correlated structural changes as the temperature is increased. The analysis was done with the averaged displacements over the temperature range as the reference spectrum. The synchronous 2D correlation spectra of the unfolding processes of the hairpins have all positive values, indicating that the mean square fluctuations of the residues become larger as the temperature is increased. The residues around the peptide ends show larger structural changes as the temperature is increased.

From the signs of the off-diagonal elements of asynchronous spectrum, one can determine the order of structural changes in the different parts of a peptide as the temperature is changed. It is assumed that the folding sequence of a peptide follows the reverse order of the temperature-induced unfolding process. Therefore, the asynchronous 2D correlation spectrum can reveal the existence of sequential events in the unfolding of a peptide.[25] Figure 7 shows the asynchronous spectra for the three hairpins. In the 1GB1 hairpin, the unfolding process is found to follow the sequence: **residues (5~9) → residues (1~4)/(10~16)**. This indicates that the formation of hydrophobic core in the strand region precedes the formation of the turn region in the folding of 1GB1, which is consistent with hydrophobic collapse mechanism.[25] As shown in Figure 7, the patterns of asynchronous spectra for the other two hairpins exhibit different behavior than that of 1GB1. For 3AIT hairpin, the analysis suggests that the unfolding sequences are: **residues (7~9)/(13~15) → residues (2~3)/(16~18) → residues (10~12: partial bend region)**. The corresponding folding process is similar to the zip-up mechanism. The asynchronous spectrum of 1A2P hairpin is consistent with the unfolding sequences of **residues (1~3)/(9~12)/(15,17) → residues (5~7)/(13~15)**. In can be argued that the formation of native structures in the strand and turn regions occurs simultaneously, which suggests the concurrent mechanism.

Concluding Remarks

We have studied the folding mechanisms of β-hairpins from proteins of 1GB1, 3AIT and 1A2P by unfolding simulations at high temperatures. The analysis of trajectories obtained from molecular dynamics simulations in explicit aqueous solution suggests that the β-hairpin structures from different proteins follow different mechanism of folding. In a recent study on the thermodynamics and kinetics of off-lattice models for the β-hairpin fragment, Klimov and Thirumalai suggested that the basic mechanisms of folding depend on the intrinsic rigidity of the hairpin, which is

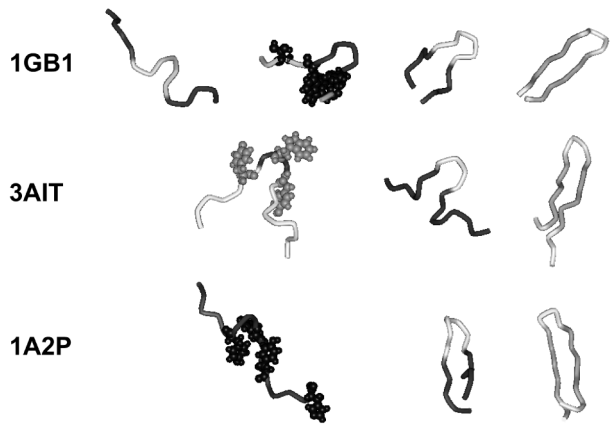

Figure 8. Snapshots of representative conformations from the unfolding simulations, showing the unfolding pathways of the three hairpins from 1GB1, 3AIT, and 1A2P. The side chains of hydrophobic residues are shown in space-filling mode.

determined by the location of the hydrophobic cluster.[36] As we discussed earlier, the positions of the hydrophobic side-chains are different in the three cases. The stability and the initial folding of the β-hairpin of protein GB1 are dominated by the formation of the hydrophobic core residues located in the middle of the two strands. The hydrophobic residues of the β-hairpin of tendamistat (3AIT) are clustered near the turn (loop) region, which facilitates the early formation of the turn and the subsequent hydrogen bond formation closing the hairpin. For the hairpin of barnase (1A2P), the hydrophobic residues do not seem to form a cluster around one region of the peptide. The best way of folding in this case would be the formation of hydrogen bonds assisted by the concomitant side-chain hydrophobic interactions. Figure 8 illustrates the folding mechanisms of the three hairpins.

In the case of 1GB1 hairpin, two conflicting folding mechanisms, the hydrophobic collapse mechanism and zip-up mechanism, have been proposed. The results of the present simulations suggested that the two models might not be totally mutually exclusive. In the process of forming the hydrophobic collapse state (*H*), which is stabilized by the interactions of hydrophobic core, there exist many intermediate structures. These intermediate structures are stabilized by the electrostatic interactions in the bend region, although the turn structures thus formed are non-native. It is possible that the final tune-up process, where the native contacts are formed, the complete hydrophobic core occurs cooperatively at the same time that the final hydrogen bonding pattern.[37,38] It may be more appropriate to propose a new mechanism of β-hairpin folding that is a blend of the hydrogen-bond-centric and the hydrophobic-centric models.

Acknowledgements. This work was supported by the Korea Research Foundation Grant through the Research Institute of Basic Science of SNU (KRF-2000-0490-20000064). SJ acknowledges the Research Professorship from the BK21 Division of Chemistry and Molecular Engineering.

References

1. Fersht, A. *Structure and Mechanism in Protein Science*; Freeman: New York, 1999.
2. Winkler, J. R.; Gray, H. B. *Acc. Chem. Res.* **1998**, *31*, 697.
3. Onuchic, J. N.; Luthey-Schulten, Z.; Wolynes, P. G. *Ann. Rev. Phys. Chem.* **1997**, *48*, 545.
4. Shakhnovich, E. I. *Curr. Opin. Struct. Biol.* **1997**, *7*, 29.
5. Dobson, C. M.; Sali, A.; Karplus, M. *Angew. Chem. Int. Ed.* **1998**, *37*, 868.
6. Dill, K. A. *Protein Sci.* **1999**, *8*, 1166.
7. Duan, Y.; Kollman, P. A. *Science* **1998**, *282*, 740.
8. Munoz, V.; Serrano, L. *Curr. Opin. Biotechnol.* **1995**, *6*, 382.
9. Thompson, P. A.; Eaton, W. A.; Hofrichter, J. *Biochemistry* **1997**, *36*, 9200.
10. Blanco, F.; Ramírez-Alvarado, M.; Serrano, L. *Curr. Opin. Struct. Biol.* **1998**, *8*, 107.
11. Chang, S.-G.; Choi, K.-D.; Kim, D.-Y.; Kang, H.-T.; Song, M.-C.; Shin, H.-C. *Bull. Korean Chem. Soc.* **2002**, *23*, 1369.
12. Munoz, V.; Thompson, P. A.; Hofrichter, J.; Eaton, W. A. *Nature* **1997**, *390*, 196.
13. Bonvin, A. M.; van Gunsteren, W. F. *J. Mol. Biol.* **2000**, *296*, 255.
14. Prevost, M.; Ortmans, I. *Proteins Struct. Funct. Genet.* **1997**, *29*, 212.
15. Pande, V. S.; Rokhsar, D. S. *Proc. Natl. Acad. Sci. USA* **1999**, *96*, 9062.
16. Dinner, A. R.; Lazaridis, T.; Karplus, M. *Proc. Natl. Acad. Sci. USA* **1999**, *96*, 9068.
17. Ma, B.; Nussinov, R. *J. Mol. Biol.* **2000**, *296*, 1091.
18. Karplus, M.; Sali, A. *Curr. Opin. Struct. Biol.* **1995**, *5*, 58.
19. Lazaridis, T.; Karplus, M. *Science* **1997**, *278*, 1928.
20. Wang, L.; Duan, Y.; Shortle, R.; Imperiali, B.; Kollman, P. A. *Protein Sci.* **1999**, *8*, 1292.
21. Finkelstein, A. V. *Protein Eng.* **1997**, *10*, 843.
22. Dinner, A. R.; Karplus, M. *J. Mol. Biol.* **1999**, *292*, 403.
23. Daggett, V. *Acc. Chem. Res.* **2002**, 35, 422.
24. Lee, J.; Shin, S. *Biophy. J.* **2001**, *81*, 2507.
25. Lee, J.; Shin, S. *J. Phys. Chem. B* **2002**, *106*, 8796.
26. Brooks, B. R.; Bruccoleri, R. E.; Olafson, B. D.; States, D. J.; Swaminathan, S.; Karplus, M. *J. Comp. Chem.* **1983**, *4*, 187.
27. Krüger, P.; Luke, M.; Szameit, A. *Comp. Phys. Comm.* **1991**, *62*, 371.
28. Wriggers, W.; Milligan, R. A.; McCammon, J. A. *J. Structural Biology* **1999**, *125*, 185.
29. Laskowski, R. A.; MacArthur, M. W.; Thornton, J. M. *J. Appl. Crystallog.* **1993**, *26*, 283.
30. Lee, J.; Lee, K.; Shin, S. *Biophy. J.* **2000**, *78*, 1665.
31. van Aalten, D. M. F.; Amadei, A.; Linssen, A. B. M.; Eijsink, V. G. H.; Vriend, G. *Proteins Struct. Funct. Genet.* **1995**, *22*, 45.
32. Vriend, G. *J. Mol. Graph.* **1990**, *8*, 52.
33. Noda, I. *Appl. Spectrosc.* **1993**, *47*, 1329.
34. Noda, I.; Dowrey, A. I.; Marcott, C.; Story, G. M.; Ozaki, Y. *Appl. Spectrosc.* **2000**, *54*, 236A.
35. Lee, J.; Suh, S. W.; Shin, S. *J. Biomol. Struct. Dyn.* **2000**, *18*, 297.
36. Klimov, D. K.; Thirumalai, D. *Proc. Natl. Acad. Sci. USA* **2000**, *97*, 2544.
37. Zagrovic, B.; Sorin, E. J.; Pande, V. *J. Mol. Biol.* **2001**, *313*, 151.
38. Zhou, R.; Berne, B. J.; Germain, R. *Proc. Natl. Acad. Sci. USA* **2001**, *98*, 14931.